

Critical Angles and Inhomogeneities in Thin Ferromagnetic Metal Films

F. Hoffmann

Laboratoire de Magnétisme, Centre National de la Recherche Scientifique, 92 Bellevue, France

(Received 5 April 1971)

The angular dependence of the intensities, linewidth, and resonance-field locations of standing spin-wave modes in thin permalloy films is precisely investigated. It is shown that each mode disappears at a specific angle. The value of this angle (measured between the normal of the film and the direction of the external magnetic field) decreases as the mode number increases. This behavior is not connected with the broadening of the linewidth and is well explained by assuming a weak inhomogeneity in the internal field. Theoretical analysis shows that the inhomogeneity is due to weak variations in the dc demagnetizing field rather than to the magnetization as generally assumed.

INTRODUCTION

A large number of papers^{1,2} have dealt with the problem of explaining the intensity and resonance-field variations of standing spin-wave modes (SSWM) in thin ferromagnetic films with the angle between the normal of the film and the applied dc magnetic field. Most of these papers¹ reported that for a given value of the angle (the "critical angle"), none of the high-order spin-wave modes were observable. A more recent paper² reports that each mode disappears for a different angle, and concludes that this disappearance is closely connected with the broadening of the linewidth.

In the present work, the angular dependence of the intensity and linewidth, as well as resonance-field locations of the spin-wave modes, is precisely investigated in permalloy films.

EXPERIMENTAL RESULTS

The permalloy films (nominally 81% Ni, 19% Fe) were prepared by evaporation onto glass slides at a pressure of 10^{-8} Torr. The resonance measurements were made using a very sensitive microwave spectrometer operating at 17.2 GHz. The samples were placed against the bottom of a TE₁₁₁ cylindrical cavity so that, as the magnet is rotated, the static and the microwave field remain mutually perpendicular.

For SSWM excited in an uniformly magnetized film, theory³ predicts that the locations of the modes should obey a dispersion relationship of the form

$$(\omega/\gamma)^2 = [H_{\text{app}} \cos(\Phi - \theta) - 4\pi M \cos^2\theta + \Lambda M k^2] \\ \times [H_{\text{app}} \cos(\Phi - \theta) - 4\pi M \cos 2\theta + \Lambda M k^2], \quad (1)$$

where ω , γ , and M have their usual meaning, Λ is the exchange constant, Φ and θ are the angles that the applied field H_{app} and the magnetization M , respectively, make with the normal of the

film. The wave number k is limited to the values $k = n\pi/d$, where d is the film thickness and n is the mode number.

In perpendicular orientation ($\Phi = 0$), the spin-wave modes are very weakly excited. The intensities of the modes are observed to alternate with mode number. The odd-numbered modes are typically about 1/50 as intense as the neighboring even-numbered modes. These facts suggest that the spins are nearly unpinning at the boundaries (in the Kittel sense⁴) and indicate a good even symmetry about the central plane of the film. The linewidth of about 40 Oe is nearly constant as a function of the mode number.⁵ The resonance fields fit quite well with the quadratic law predicted by Eq. (1) except for the first modes (typically the two first modes for a film of 3730-Å thickness, see Fig. 4).

A careful analysis of the position data shows that, for the main resonance, the Φ dependence of the applied field is very close to that predicted for a uniform resonance for $4\pi M = 10590$ G and $g = 2.08$. To fit the data of the high-order modes with Eq. (1) however, it is necessary to assume a dependence of the wave number versus the angle Φ .

As the linewidth ΔH_n varies with the angle Φ , the measured amplitudes must be multiplied by the linewidth in order to obtain the intensity of excitation of the modes. Figure 1 shows these excitations versus the angle Φ for the modes 6, 8, and 10 of a typical film of thickness about 3730 Å. The modes of order 2 and 4 overlap with the main resonance mode and cannot provide a precise measurement of the intensities. The modes of order higher than 10 cannot be observed for large θ because of the weakness of their resonance fields.

Each mode disappears at a given angle and this angle, called the critical angle, decreases as the wave number increases. This behavior is not connected with the broadening in the linewidth; in

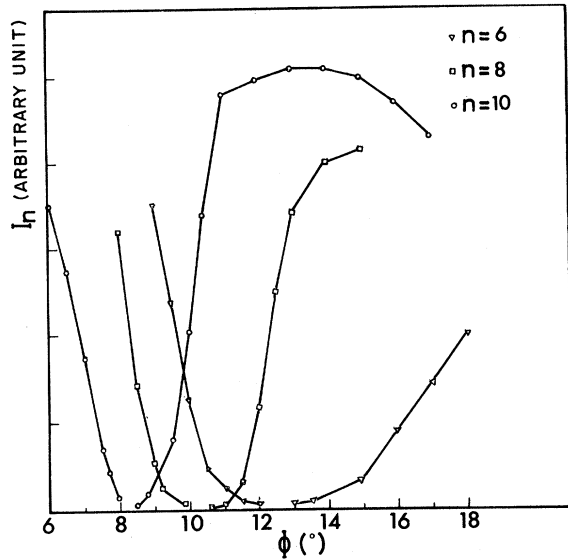


FIG. 1. Intensity I_n of the modes 6, 8, and 10 of a typical film vs the angle Φ between the applied field and the normal to the film. The value of the critical angle increases as the mode number decreases.

fact the linewidth increases and reaches a maximum for an angle larger than the critical angle. As an example, Fig. 2 shows that for $n=10$ the critical angle is $\Phi \approx 8.2^\circ$ when the maximum of the linewidth occurs at $\Phi \approx 11.8^\circ$.

THEORETICAL INTERPRETATION

The experimental results are interpreted by assuming a weak inhomogeneity in the internal dc magnetic field. An inhomogeneous internal magnetic field could arise either from an inhomogeneous magnetization or from an inhomogeneous demagnetizing field due to the surface roughness. A variation in the magnetization can be due to oxide inclusions whose density increases as the surfaces are approached.⁶ Changing the composition of the alloy across the thickness also gives an inhomogeneous M_s .⁷ On the other hand, surface structural irregularities produce weaker demagnetizing field near the surfaces of the film and the long-range nature of the dipole interaction will give rise to a change in the field at large distances from the surface.^{8,9}

An approximate calculation based on the WKB methods gives the locations of the modes and a very simple expression for the mode intensities.

After linearization and diagonalization, the equation of motion of the magnetization can be written as¹⁰

$$\frac{\partial^2 m}{\partial z^2} + H_{\text{eff}} m = 0,$$

where $m = m_x + imy/\alpha$ is the linear combination of m_x and m_y obtained from the diagonalization and

$$H_{\text{eff}} = (1/M\Lambda) \{ [(2\pi M \sin^2\theta)^2 + (\omega/\gamma)^2]^{1/2} - H_{\text{av}} \cos(\theta - \Phi) + h_D + \Lambda \nabla^2 M - 2\pi M \sin^2\theta \}. \quad (2)$$

In this expression for H_{eff} , h_D is the component of the dc demagnetizing field along the direction of the internal field (i. e., $h_D = 4\pi M \cos^2\theta$ for perfect films). The z axis is in the direction perpendicular to the film surfaces.

To estimate the effect of the variation of H_{eff} , it is convenient to write the effective field as follows:

$$H_{\text{eff}}(z) = \langle H_{\text{eff}} \rangle - \delta H_{\text{eff}}(z),$$

where $\langle H_{\text{eff}} \rangle$ is the mean value and $\delta H_{\text{eff}}(z)$ describes the fluctuations of the effective field.

For small $\delta H_{\text{eff}}/\langle H_{\text{eff}} \rangle$, and with unpinned boundary conditions, the locations of the modes are shown to be¹¹

$$\langle H_{\text{eff}} \rangle = n^2 \pi^2 / d^2. \quad (3)$$

In the circular-precession approximation, the mode excitation I_n is evaluated in increasing power of the inhomogeneity $\delta H_{\text{eff}}/\langle H_{\text{eff}} \rangle$. The first-order term is proportional to

$$\left| \int_0^d \frac{\delta H_{\text{eff}}}{\langle H_{\text{eff}} \rangle} \cos \frac{n\pi z}{d} dz \right|^2. \quad (4)$$

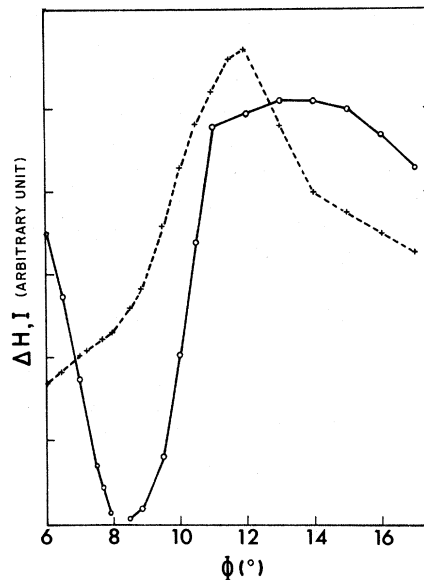


FIG. 2. Intensity I_n , indicated by the symbol \circ , and linewidth ΔH , indicated by the symbol \triangle , are shown for mode 10 vs angle Φ . The positions of the critical angle and maximum linewidth are different.

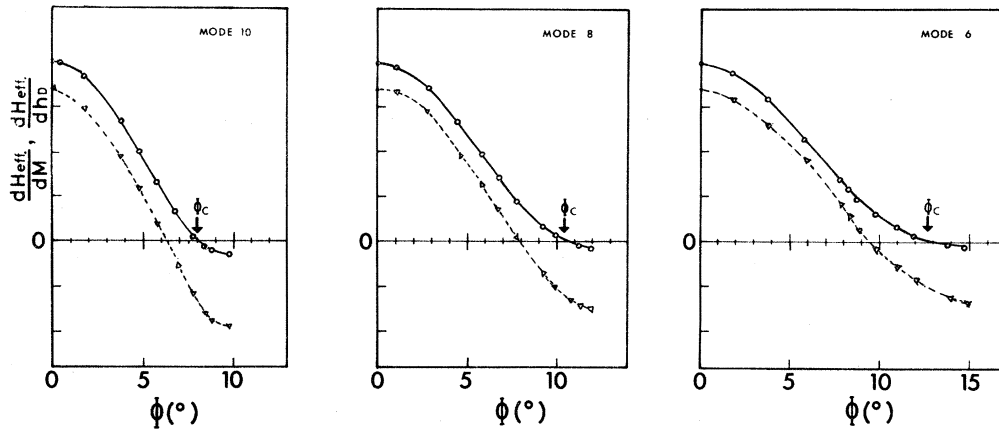


FIG. 3. Calculated angular dependence of the quantities $\partial H_{\text{eff}}/\partial M$, indicated by the symbol ∇ , and $\partial H_{\text{eff}}/\partial h_D$, indicated by the symbol \circ , vs angle Φ for the film used in Figs. 1 and 2. For the calculation, H_{app} and Φ are the experimental values; the values $4\pi M = 10\,590$ G and $g = 2.08$ are obtained from the variation of the main resonance location versus Φ . The arrows indicate the values of the experimental critical angles.

The influence of the ellipticity of the precession on this expression is discussed in the Appendix. The n th-mode intensity vanishes with the n th Fourier component of δH_{eff} . The value of the angle Φ at which this phenomenon occurs is generally dependent on the shape and magnitude of the inhomogeneity. However for a weak inhomogeneity with a characteristic length of variation of the order or larger than the film thickness, the Fourier component vanishes only if δH_{eff} vanishes and the critical angles are no longer dependent on the particular shape of the inhomogeneity. With these hypotheses, the critical angles can be found by differentiating the effective field and solving for $\partial H_{\text{eff}}/\partial M = 0$ in the case of an inhomogeneous magnetization, or $\partial H_{\text{eff}}/\partial h_D = 0$ in the case of a demagnetizing-field inhomogeneity.

Figure 3 shows the quantities proportional to $\partial H_{\text{eff}}/\partial M$ and $\partial H_{\text{eff}}/\partial h_D$ calculated with the experimental values of Φ and H_{app} . For both cases the calculated values of the critical angles decrease as the mode number increases. The experimental values are very close to the calculated one with the assumption of an inhomogeneous demagnetizing field.

The shape of H_{eff} is dependent on the angle and on the magnetic field strength, so that for any angle the location of the modes cannot be calculated without supplementary assumptions on the inhomogeneity.

In the perpendicular orientation, Eq. (3) reduces to

$$\left\langle \frac{(\omega/\gamma) + h_D - H_{\text{app}}}{M\Lambda} \right\rangle = \frac{n^2\pi^2}{d^2},$$

and with the assumption that only the demagnetizing field is varying, to

$$H_{\text{app}} = \frac{\omega}{\gamma} + \langle h_D \rangle - \frac{M\Lambda n^2\pi^2}{d^2}.$$

Thus an upper limiting value of the magnitude of the inhomogeneity is given by the difference between the main peak field and the field where deviation from the quadratic spacing behavior occurs. As can be seen in Fig. 4, this value is typically of the order of a few hundred Oersteds.

At the critical angles, the effective fields are independent of small change in the demagnetizing field so that the quantities $M\Lambda n^2\pi^2/d^2$ can be directly evaluated. The quantities so determined fit the quadratic law extremely well, and the data plotted versus the square of the mode number intercept the axis at the origin (Fig. 4). It is noticeable that the linear part of $H_0 - H_n$ and the $M\Lambda n^2\pi^2/d^2$ line exhibit rigorously the same slope. The separation between the two lines is 140 Oe. The fact that the two lines in Fig. 4 are parallel also supports the evidence that the variation in the internal field is due to a variation in the demagnetization field rather than in the magnetization itself, for Sparks has shown that for a variation⁸ in the magnetization, the slope would be different from that for the case of an inhomogeneous demagnetization. At the critical angle the internal field is homogeneous and a "true" dispersion law should be obeyed. At perpendicular resonance, the inhomogeneous demagnetization field will give a "true" dispersion law while an inhomogeneous magnetization gives a "dressed" dispersion law where the slope in Fig. 4 would be increased slightly.

CONCLUSION

Several series of permalloy films of different

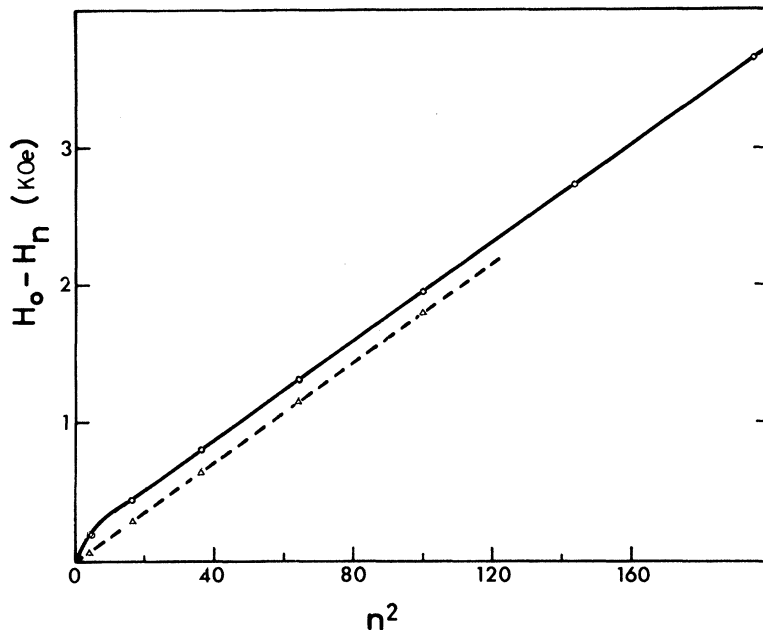


FIG. 4. Magnetic field difference, $H_0 - H_n$, between the main peak and the high-order mode vs the square of the mode number in perpendicular resonance represented by open circles. The data deviate from the quadratic law for the first two modes. The dels (Δ) represent the quantities $M\Lambda n^2 \pi^2 / d^2$ deduced for the location of the modes at the critical angles. This line is parallel to the linear part of the $H_0 - H_n$ curve. The separation between the lines is 140 Oe.

thicknesses have been used for this rotation experiment. Without exception, every film exhibits the same behavior. The observed values for the critical angles suggest that the main source of inhomogeneity is the imperfections of the surfaces rather than a variation in the magnetization.

As pointed out by Sparks,⁸ the amount of surface roughness depends on the size of the crystallites, the surface being quite smooth over a large fraction of the area of the film when the cross-section sizes of the crystallites are larger than the film thickness. For the films studied in the present work, the cross-sectional dimensions of the crystallites are typically of the order of 500 Å. It would be interesting to repeat these experiments for films having larger crystallite sizes. This work, to be performed on epitaxial films, is in progress.

ACKNOWLEDGMENTS

The author would like to express his sincere thanks to P. Couranjou for assistance in film preparation. Thanks are also due H. Pascard

for helpful discussions.

APPENDIX

In the experimental arrangements, the microwave field used to excite the modes is linearly polarized, so that the relative intensities of the modes for constant ω are given by the expression¹²

$$I_n = \left| \int_0^d m_y dz \right|^2 / \int_0^d |m|^2 dz.$$

In the perpendicular configuration, or in the circular-precession approximation, the ratio of $m_{x,y}$ to m is the same for every mode; however, that is not generally the case.

Taking into account the ellipticity, formula (4) is modified as follows:

$$I_n \propto \left| \int_0^d \alpha (1 + \delta H_{\text{eff}} / \langle H_{\text{eff}} \rangle) \cos n\pi z dz \right|^2.$$

The correction on the critical angles is very small and can be neglected in the present analysis.

¹P. E. Wigen, C. F. Kooi, M. R. Shanabarger, U. K. Cummings, and M. E. Baldwin, *J. Appl. Phys.* **34**, 1137 (1963); P. E. Wigen, C. F. Kooi, M. R. Shanabarger, and T. D. Rossing, *Phys. Rev. Letters* **9**, 206 (1962); T. D. Rossing, *J. Appl. Phys.* **34**, 1133 (1963); M. Nisenoff and R. W. Terhune, *ibid.* **36**, 732 (1965).

²Makoto Okochi and Korski Nose, *J. Phys. Soc. Japan* **27**, 312 (1969).

³R. F. Soohoo, *Phys. Rev.* **131**, 594 (1963).

⁴C. Kittel, *Phys. Rev.* **110**, 1295 (1958).

⁵H. Pascard and F. Hoffmann, *Phys. Status Solidi* **4**,

K-59 (1971).

⁶A. M. Portis, *Appl. Phys. Letters* **2**, 69 (1963).

⁷C. F. Kooi, P. E. Wigen, M. R. Shanabarger, and J. Kerrigan, *J. Appl. Phys.* **35**, 791 (1964).

⁸M. Sparks, *Solid State Commun.* **8**, 659 (1970).

⁹E. Schlomann and R. J. Joseph, *J. Appl. Phys.* **41**, 1336 (1970).

¹⁰M. Sparks, *Phys. Rev. Letters* **22**, 1111 (1969).

¹¹F. Hoffmann, *Solid State Commun.* **9**, 299 (1971).

¹²M. Sparks, *Phys. Rev. B* **1**, 3869 (1970).